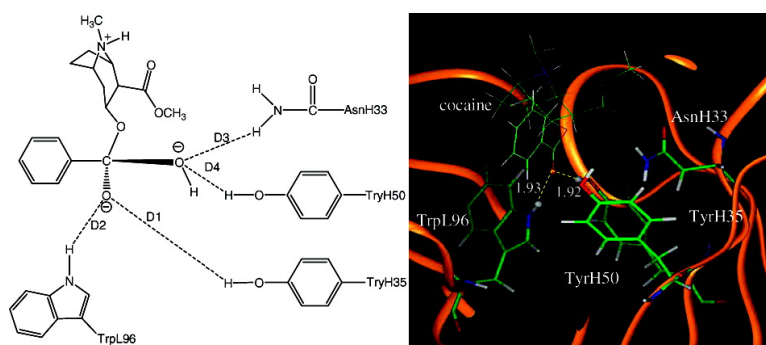


Modeling the Catalysis of Anti-Cocaine Catalytic Antibody: Competing Reaction Pathways and Free Energy Barriers

Yongmei Pan, Daquan Gao, and Chang-Guo Zhan

J. Am. Chem. Soc., **2008**, 130 (15), 5140-5149 • DOI: 10.1021/ja077972s • Publication Date (Web): 15 March 2008

Downloaded from <http://pubs.acs.org> on February 8, 2009



More About This Article

Additional resources and features associated with this article are available within the HTML version:

- Supporting Information
- Links to the 1 articles that cite this article, as of the time of this article download
- Access to high resolution figures
- Links to articles and content related to this article
- Copyright permission to reproduce figures and/or text from this article

[View the Full Text HTML](#)

Modeling the Catalysis of Anti-Cocaine Catalytic Antibody: Competing Reaction Pathways and Free Energy Barriers

Yongmei Pan, Daquan Gao, and Chang-Guo Zhan*

Department of Pharmaceutical Sciences, College of Pharmacy, University of Kentucky, 725 Rose Street, Lexington, Kentucky 40536

Received October 17, 2007; E-mail: zhan@uky.edu

Abstract: The competing reaction pathways and the corresponding free energy barriers for cocaine hydrolysis catalyzed by an anti-cocaine catalytic antibody, mAb15A10, were studied by using a novel computational strategy based on the binding free energy calculations on the antibody binding with cocaine and transition states. The calculated binding free energies were used to evaluate the free energy barrier shift from the cocaine hydrolysis in water to the antibody-catalyzed cocaine hydrolysis for each reaction pathway. The free energy barriers for the antibody-catalyzed cocaine hydrolysis were predicted to be the corresponding free energy barriers for the cocaine hydrolysis in water plus the calculated free energy barrier shifts. The calculated free energy barrier shift of -6.87 kcal/mol from the dominant reaction pathway of the cocaine benzoyl ester hydrolysis in water to the dominant reaction pathway of the antibody-catalyzed cocaine hydrolysis is in good agreement with the experimentally derived free energy barrier shift of -5.93 kcal/mol. The calculated mutation-caused shifts of the free energy barrier are also reasonably close to the available experimental activity data. The good agreement suggests that the protocol for calculating the free energy barrier shift from the cocaine hydrolysis in water to the antibody-catalyzed cocaine hydrolysis may be used in future rational design of possible high-activity mutants of the antibody as anti-cocaine therapeutics. The general strategy of the free energy barrier shift calculation may also be valuable in studying a variety of chemical reactions catalyzed by other antibodies or proteins through noncovalent bonding interactions with the substrates.

Introduction

As is well-known, cocaine abuse and addiction are major medical and public health problems in our society. The disastrous medical consequences of reinforcing and toxic effects of cocaine have made the development of an anti-cocaine medication a high priority. It is commonly believed that dopamine transporter (DAT), a protein that brings synaptic dopamine back to the presynaptic neuron (dopamine reuptake), is responsible for the rewarding effects of cocaine. Cocaine mediates its reinforcing and toxic effects by blocking the reuptake of neurotransmitter dopamine. By binding to DAT, cocaine increases the concentration of synaptic dopamine and produces such feelings as reward and pleasure.¹⁻⁴ On the basis of the pharmacology, a pharmacodynamic approach was used to design small molecules such as DAT inhibitors and dopamine receptor antagonists to decrease cocaine toxicity.^{1,2,4} However, the classical pharmacodynamic approach has failed to yield a clinically useful small-molecule inhibitor/antagonist due to the difficulties inherent in blocking a blocker.^{1,4} An alternative to the pharmacodynamic approach is the pharmacokinetic approach, which means finding an enzyme or antibody to prevent cocaine from crossing the brain-blood barrier. The pharma-

cokinetic approach is recognized as the most promising strategy for the development of anti-cocaine medication and, therefore, has received more and more attention.^{1,2,4,5} One way of this approach is to design a catalytic antibody that catalyzes cocaine metabolism through hydrolysis. The catalytic antibodies are considered as a class of artificial enzymes.

Various anti-cocaine catalytic antibodies have been developed.⁶⁻⁸ Of all anti-cocaine catalytic antibodies reported in the literature so far, monoclonal antibody (mAb) 15A10^{6,9} has the highest catalytic activity with $K_M = 220 \mu\text{M}$ and $k_{\text{cat}} = 2.3 \text{ min}^{-1}$. This catalytic antibody was elicited from a stable structural analogue of the transition state for cocaine hydrolysis in aqueous solution at physiologic pH (7.4), that is, the hydroxide ion-catalyzed hydrolysis of cocaine. Antibody 15A10 catalyzes the hydrolysis of cocaine benzoyl ester to produce two biologically inactive metabolites, that is, ecgonine methyl ester and benzoyl acid, and gives a rate acceleration of $k_{\text{cat}}/k_0 = 23\,000$ (k_{cat} is the catalytic rate constant for the antibody-catalyzed hydrolysis of cocaine at the benzoyl ester; k_0 is the

- (1) Gorelick, D. A.; Gardner, E. L.; Xi, Z. X. *Drugs* **2004**, *64*, 1547.
- (2) See: <http://ibogaine.mindvox.com/index.html?Media/Lancet01.html~mainframe>.
- (3) Johanson, C. E.; Fischman, M. W. *Pharmacol. Rev.* **1989**, *41*, 3.
- (4) Carroll, F. I.; Howell, L. L.; Kuhar, M. J. *J. Med. Chem.* **1999**, *42*, 2721.

- (5) Gorelick, D. A. *Drug Alcohol Depend.* **1997**, *48*, 159.
- (6) Larsen, N. A.; de Prada, P.; Deng, S. X.; Mittal, A.; Brskett, M.; Zhu, X.; Wilson, I. A.; Landry, D. W. *Biochemistry* **2004**, *43*, 8067.
- (7) Pozharski, E.; Moulin, A.; Hewagama, A.; Shanafelt, A. B.; Petsko, G. A.; Ringe, D. *J. Mol. Biol.* **2005**, *349*, 570.
- (8) Zhu, X.; Dickerson, T. J.; Rogers, C. J.; Kaufmann, G. F.; Mee, J. M.; McKenzie, K. M.; Janda, K. D.; Wilson, I. A. *Structure* **2006**, *14*, 205.
- (9) Landry, D. W. Anti-cocaine catalytic antibody. United States Patent No. 6913917, 2005.

first-order rate constant for the spontaneous hydrolysis of the cocaine benzoyl ester, that is, the hydrolysis of cocaine benzoyl ester in water). Previous studies showed that mAb15A10 blocked the reinforcing effect of cocaine self-administration in rat models^{10,11} and reduced cocaine-induced seizures and deaths in a dose-dependent manner.¹⁰ However, the catalytic efficiency of mAb15A10 is still so low that an extremely high dose of the antibody (15–50 mg/kg) would be needed to produce the desirable protective effects.¹² It is highly desirable to design a high-activity mutant of the catalytic antibody with a significantly improved catalytic efficiency (k_{cat}/K_M) or catalytic rate constant (k_{cat}). As demonstrated in other protein engineering efforts,^{13–19} an appropriate computational enzyme mutant design, followed by site-directed mutagenesis and catalytic activity tests, could eventually lead to discovery of an enzyme mutant with a sufficiently higher catalytic efficiency against cocaine.

To rationally design a high-activity mutant of the catalytic antibody, one first needs to understand the detailed mechanism concerning how the antibody catalyzes hydrolysis of cocaine and develop a reliable computational strategy and protocol to evaluate the free energy barrier for the antibody-catalyzed hydrolysis of cocaine. Concerning the catalytic mechanism of the antibody-catalyzed hydrolysis of cocaine, the reported X-ray crystal structure of mAb15A10⁶ did not show a nucleophile which attacks the carbonyl carbon of cocaine to initialize the cocaine hydrolysis, although the X-ray crystal structure did suggest that three amino acid residues (i.e., TrpL96, AsnH33, and TyrH35) likely form an oxyanion hole in a shallow binding pocket. On the basis of the X-ray crystal structure, the mechanism for the antibody-catalyzed hydrolysis of cocaine should be completely different from those known for the ester hydrolysis catalyzed by an esterase. The catalytic antibody only can bind with cocaine during the cocaine hydrolysis process, without changing the fundamental reaction pathways for the cocaine hydrolysis in aqueous solution. As the dominant reaction pathway for cocaine hydrolysis in aqueous solution is associated with the hydroxide ion-catalyzed cocaine hydrolysis, the most likely mechanism of the antibody-catalyzed cocaine hydrolysis is that the catalytic antibody helps to stabilize the transition state for the rate-determining step of the hydroxide ion-catalyzed cocaine hydrolysis. See Figure 4 for the schematic representations of cocaine and the transition state structures binding with mAb15A10.

Further, our recently reported first-principles reaction coordinate calculations^{20,21} on the cocaine hydrolysis demonstrated three competing reaction pathways for the hydroxide ion-

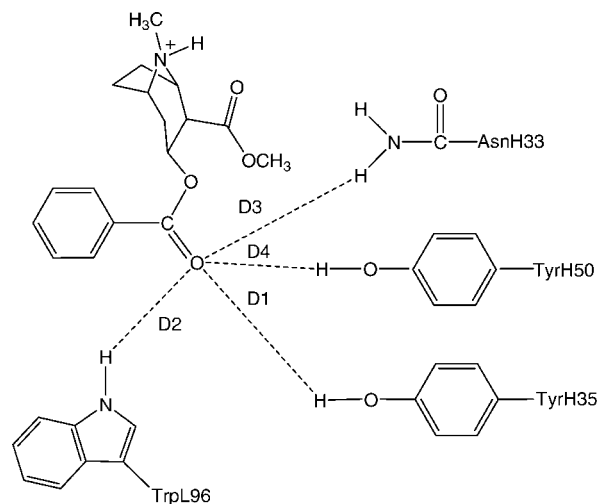


Figure 1. Schematic representation of cocaine binding with the antibody. The dashed lines refer to the key distances between cocaine and the antibody.

catalyzed cocaine hydrolysis in water: two pathways correspond to the hydrolysis of cocaine at the benzoyl ester, whereas the other pathway corresponds to the hydrolysis of cocaine at the methyl ester. The pathway corresponding to the cocaine methyl ester hydrolysis has the lowest free energy barrier in water, which is consistent with the experimental kinetics.²² Obviously, mAb15A10 should not be expected to equally stabilize the transition states for all of the competing reaction pathways. It is likely that this catalytic antibody more favorably stabilizes the transition state for one of the competing reaction pathways associated with the hydrolysis of cocaine at the benzoyl ester.

In order to identify the most favorable reaction pathway for the antibody-catalyzed cocaine hydrolysis and to better understand the catalysis of the catalytic antibody, in the present study, we have developed a novel computational strategy to calculate the free energy barriers for the competing reaction pathways of the antibody-catalyzed cocaine hydrolysis. According to the computational strategy, we first carried out molecular docking, molecular dynamics (MD) simulations, and binding free energy calculations to study how the antibody binds with cocaine and the transition-state structures determined by the first-principles reaction coordinate calculations on the competing reaction pathways. The calculated binding free energies, along with the free energy barriers determined by the first-principles reaction coordinate calculations on the hydroxide ion-catalyzed cocaine hydrolysis in water, lead to the computational predictions of the free energy barriers of the antibody-catalyzed cocaine hydrolysis for all of the three competing reaction pathways, thus enabling us to determine the dominant reaction pathway for the antibody-catalyzed cocaine hydrolysis. The calculated energetic results are in good agreement with available experimental kinetic data, suggesting that the computational strategy and protocol are reliable for studying the reaction pathways and free energy barriers for the antibody-catalyzed cocaine hydrolysis and other antibody-catalyzed reactions.

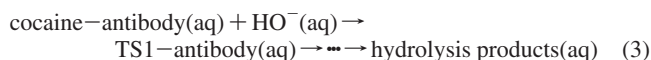
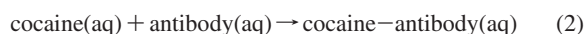
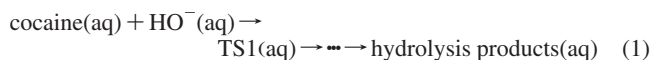
Computational Methods

General Computational Strategy. As is well-known, direct reaction coordinate calculations on a reaction system involving a

- (10) Mets, B.; *Proc. Natl. Acad. Sci. U.S.A.* **1998**, *95*, 10176.
- (11) Baird, T. J.; Deng, S. X.; Landry, D. W.; Winger, G.; Woods, J. H. *J. Pharmacol. Exp. Ther.* **2000**, *295*, 1127.
- (12) Cooper, Z. D.; Narasimhan, D.; Sunahara, R. K.; Mierzejewski, P.; Jutkiewicz, E. M.; Larsen, N. A.; Wilson, I. A.; Landry, D. W.; Woods, J. H. *Mol. Pharmacol.* **2006**, *70*, 1885.
- (13) Zhan, C.-G.; Zheng, F.; Landry, D. W. *J. Am. Chem. Soc.* **2003**, *125*, 2462.
- (14) Gao, D. Q.; Zhan, C.-G. *J. Phys. Chem. B* **2005**, *109*, 23070.
- (15) Hamza, A.; Cho, H.; Tai, H. H.; Zhan, C.-G. *J. Phys. Chem. B* **2005**, *109*, 4776.
- (16) Pan, Y. M.; Gao, D. Q.; Yang, W. C.; Cho, H.; Yang, G. F.; Tai, H. H.; Zhan, C.-G. *Proc. Natl. Acad. Sci. U.S.A.* **2005**, *102*, 16656.
- (17) Zhan, C. G.; Gao, D. Q. *Biophys. J.* **2005**, *89*, 3863.
- (18) Gao, D.; Cho, H.; Yang, W.; Pan, Y.; Yang, G.; Tai, H. H.; Zhan, C. G. *Angew. Chem., Int. Ed.* **2006**, *45*, 653.
- (19) Gao, D. Q.; Zhan, C.-G. *Proteins* **2006**, *62*, 99.
- (20) Zhan, C.-G.; Deng, S. X.; Skiba, J. G.; Hayes, B. A.; Tschampel, S. M.; Shields, G. C.; Landry, D. W. *J. Comput. Chem.* **2005**, *26*, 980.
- (21) Zhan, C. G.; Landry, D. W. *J. Phys. Chem. A* **2001**, *105*, 1296.

- (22) Li, P.; Zhao, K.; Deng, S. X.; Landry, D. W. *Helv. Chim. Acta* **1999**, *82*, 85.

protein or antibody (which is considered to be an artificial protein) and the predictions of the corresponding free energy barriers would be very time-consuming. To simplify the calculations of the free energy barriers for the antibody-catalyzed hydrolysis of cocaine, we consider the following reaction systems:



Reaction 1 is the hydroxide ion-catalyzed hydrolysis of cocaine in aqueous solution without the antibody. In reaction 1, cocaine(aq) and HO[−](aq) represent the solvated cocaine molecule and solvated hydroxide ion, respectively. TS1(aq) refers to the transition state for the first step, which is the rate-determining step, of the hydroxide ion-catalyzed cocaine hydrolysis in aqueous solution without the antibody. The free energy barrier (or the activation free energy), Δ*G*_{av}(aq), for reaction 1 is calculated as the Gibbs free energy change from cocaine(aq) + HO[−](aq) to TS1(aq):

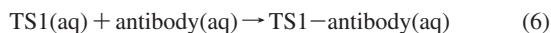
$$\Delta G_{\text{av}}(\text{aq}) = G[\text{TS1(aq)}] - G[\text{cocaine(aq)}] - G[\text{HO}^{\ominus}(\text{aq})] \quad (4)$$

Three competing reaction pathways were uncovered in our recently reported first-principles reaction coordinate calculations^{20,21} on the hydroxide ion-catalyzed hydrolysis of cocaine in water (at the B3LYP/6-31+G* level for the entire cocaine molecule with HO[−]). The rate-determining transition states for these three competing reaction pathways are denoted by TS1_{ben-Re}, TS1_{ben-Si}, and TS1_{met} (see Figure 4). TS1_{met} is the transition state for the hydroxide ion-catalyzed hydrolysis of cocaine at the methyl ester. For the hydroxide ion-catalyzed hydrolysis of cocaine at the benzoyl ester, the nucleophilic hydroxide ion can approach from two faces, denoted by Si and Re, of the carbonyl to form two stereoisomer tetrahedral intermediates (*R* and *S*) through two different transition-state structures, denoted by TS1_{ben-Re} and TS1_{ben-Si}, respectively. The free energy barrier was calculated for each reaction pathway at the high level of first-principles electronic structure calculations that accurately account for the solvation effects by using our recently developed fully polarizable continuum model (FPCM).^{23–27}

Reactions 2 and 3 represent the antibody-catalyzed hydrolysis of cocaine. In reactions 2 and 3 taking place in aqueous solution, cocaine-antibody(aq) represents the complex between the antibody and the cocaine molecule, whereas TS1-antibody(aq) refers to the complex between the antibody and the rate-determining transition state of cocaine hydrolysis. Hence, reaction 2 refers to the binding of cocaine to the antibody, whereas reaction 3 represents the chemical reaction process starting from the cocaine-antibody binding complex (i.e., cocaine-antibody(aq)). The free energy barrier for the antibody-catalyzed hydrolysis of cocaine can be evaluated as the Gibbs free energy change from the cocaine-antibody(aq) + HO[−](aq) to TS1-antibody(aq):

$$\Delta G_{\text{av}}(\text{antibody}) = G[\text{TS1-antibody(aq)}] - G[\text{cocaine-antibody(aq)}] - G[\text{HO}^{\ominus}(\text{aq})] \quad (5)$$

Further, let us consider the binding between the antibody and the rate-determining transition state TS1:



The Gibbs free energy changes of reactions 2 and 6 give

$$\Delta G_{\text{bind}}(\text{cocaine, aq}) = G[\text{cocaine-antibody(aq)}] - G[\text{cocaine(aq)}] - G[\text{antibody(aq)}] \quad (7)$$

$$\Delta G_{\text{bind}}(\text{TS1, aq}) = G[\text{TS1-antibody(aq)}] - G[\text{TS1(aq)}] - G[\text{antibody(aq)}] \quad (8)$$

where Δ*G*_{bind}(cocaine, aq) is the binding free energy for cocaine binding with the antibody and Δ*G*_{bind}(TS1, aq) is the binding free energy for the rate-determining transition state (TS1) binding with the antibody.

Further, a combination of eqs 4 and 5 gives

$$\Delta G_{\text{av}}(\text{antibody}) - \Delta G_{\text{av}}(\text{aq}) = G[\text{TS1-antibody(aq)}] - G[\text{cocaine-antibody(aq)}] - G[\text{TS1(aq)}] + G[\text{cocaine(aq)}] \quad (9)$$

Equations 7 and 8 give

$$\Delta G_{\text{bind}}(\text{TS1, aq}) - \Delta G_{\text{bind}}(\text{cocaine, aq}) = G[\text{TS1-antibody(aq)}] - G[\text{TS1(aq)}] - G[\text{cocaine-antibody(aq)}] + G[\text{cocaine(aq)}] \quad (10)$$

Comparing eq 9 with eq 10, we have Δ*G*_{av}(antibody) − Δ*G*_{av}(aq) = Δ*G*_{bind}(TS1, aq) − Δ*G*_{bind}(cocaine, aq) or

$$\Delta G_{\text{av}}(\text{antibody}) = \Delta G_{\text{av}}(\text{aq}) + \Delta G_{\text{bind}}(\text{TS1, aq}) - \Delta G_{\text{bind}}(\text{cocaine, aq}) \quad (11)$$

$$\begin{aligned} \Delta \Delta G_{\text{av}} &\equiv \Delta G_{\text{av}}(\text{antibody}) - \Delta G_{\text{av}}(\text{aq}) \\ &= \Delta G_{\text{bind}}(\text{TS1, aq}) - \Delta G_{\text{bind}}(\text{cocaine, aq}) \end{aligned} \quad (12)$$

Reactions 11 and 12 indicate that the free energy barrier shift, ΔΔ*G*_{av}, from the cocaine hydrolysis in water to the antibody-catalyzed cocaine hydrolysis is equal to the binding free energy change from the cocaine-antibody binding to the TS1-antibody binding. Because we have already known the free energy barriers, that is, the Δ*G*_{av}(aq) values, for the cocaine hydrolysis in water based on our previous first-principles reaction coordinate calculations, the task of the free energy barrier calculations on the antibody-catalyzed hydrolysis processes can be simplified as the calculations of the binding free energies, that is, Δ*G*_{bind}(cocaine, aq) and Δ*G*_{bind}(TS1, aq), for the antibody binding with cocaine and the transition states.

Further, even without knowing Δ*G*_{av}(aq), the calculated ΔΔ*G*_{av} value can be used to estimate the ratio (*k*_{cat}/*k*₀) of the catalytic rate constant *k*_{cat} for the antibody-catalyzed cocaine hydrolysis to the rate constant *k*₀ of the corresponding cocaine hydrolysis in water by using the conventional transition state theory (CTST):²⁸

$$k_{\text{cat}}/k_0 = (k_{\text{B}}T/h)\exp(-\Delta \Delta G_{\text{av}}/k_{\text{B}}T) \quad (13)$$

where *k*_B is the Boltzmann constant, *T* is the absolute temperature, and *h* is Planck's constant. In addition, the calculated Δ*G*_{bind}(cocaine, aq) value can be used to evaluate the dissociation constant (*K*_d) for the cocaine-antibody binding:

$$\Delta G_{\text{bind}}(\text{cocaine, aq}) = -RT \times \ln K_{\text{d}} \quad (14)$$

The calculated *K*_d can be compared to the reported Michaelis-Menten constant (*K*_M), as *K*_M ≈ *K*_d under the rapid equilibrium assumption.^{29,30}

For each reaction pathway, the binding free energies Δ*G*_{bind}(cocaine, aq) and Δ*G*_{bind}(TS1, aq) were calculated by performing molecular docking of our previously optimized structures of cocaine and TS1 to mAb15A10, followed by molecular dynamics (MD) simulations and binding free energy calculations on the docked cocaine-antibody and TS1-antibody complexes in a water bath. An implicit approximation used here is that the TS1 structure in

(23) Zhan, C. G.; Bentley, J.; Chipman, D. M. *J. Chem. Phys.* **1998**, *108*, 177.

(24) Zhan, C. G.; Chipman, D. M. *J. Chem. Phys.* **1998**, *109*, 10543.

(25) Zhan, C. G.; Chipman, D. M. *J. Chem. Phys.* **1999**, *110*, 1611.

(26) Zhan, C. G.; Landry, D. W.; Ornstein, R. L. *J. Phys. Chem. A* **2000**, *104*, 7672.

(27) Chen, X.; Zhan, C. G. *J. Phys. Chem. A* **2004**, *108*, 6407.

(28) Alvarez-Idaboy, J. R.; Galano, A.; Bravo-Perez, G.; Ruiz, M. E. *J. Am. Chem. Soc.* **2001**, *123*, 8387.

(29) Anderson, W. B.; Board, P. G.; Anders, M. W. *Chem. Res. Toxicol.* **2004**, *17*, 650.

(30) Houston, J. B.; Galetin, A. *Arch. Biochem. Biophys.* **2005**, *433*, 351.

the presence of the antibody is assumed to be the same as that in the absence of the antibody. Below, we describe the computational details.

Molecular Docking and Molecular Dynamics Simulation.

Molecular docking and molecular dynamics (MD) simulations were carried out to determine the best possible binding mode for mAb15A10 binding with each "ligand", such as cocaine, TS1_{ben}-Re, TS1_{ben}-Si, or TS1_{met}. The initial structure of mAb15A10 used in our molecular docking and MD simulations came from the X-ray crystal structure (1NJ9) deposited in the Protein Data Bank.³¹ Since the crystal structure is a dimer, two of the four chains (i.e., the high (H) and low (L) chains) were used to build the antibody structure (monomer). The initial structures of cocaine and the transition states (i.e., TS1_{ben}-Re, TS1_{ben}-Si, and TS1_{met}) used were the geometries optimized at the B3LYP/6-31+G* level as reported in our previous first-principles reaction coordinate calculations on the reaction system consisting of cocaine and hydroxide ion.²⁰ The optimized geometry of cocaine is associated with a local minimum on the potential energy surface, whereas the optimized geometries of the transition states are associated with first-order saddle points on the potential energy surface. The geometries optimized at the B3LYP/6-31+G* level were used, in the present study, to perform ab initio electronic structure calculations at the HF/6-31G* level using the Gaussian03 program³² and to determine the electrostatic potentials at points selected according to the Merz-Singh-Kollman scheme.^{33,34} On the basis of the calculated electrostatic potential, the restrained electrostatic potential (RESP) protocol^{35,36} implemented in the Antechamber module of the Amber8³⁷ program was used to calculate the RESP charges required for the molecular docking and MD simulations with cocaine, TS1_{ben}-Re, TS1_{ben}-Si, and TS1_{met}.

Molecular docking with each ligand, such as cocaine, TS1_{ben}-Re, TS1_{ben}-Si, or TS1_{met}, was performed by using AutoDock program version 3.0.³⁸ For the ligands, all flexible torsion angles were allowed to rotate during the docking, while all of the bond lengths and angles were fixed. During the docking process, the Lamarckian genetic algorithm (LGA)³⁸ was applied to the conformational search for the antibody-ligand binding structure. Among a series of docking parameters, the grid size used in the docking was 60 × 60 × 60, and the used grid space was the default value of 0.375 Å.³⁹ For molecular docking with each ligand, the best binding structure with the most intermolecular hydrogen bonds (see Figure 4) was selected as the initial structure of the antibody-ligand complex for MD simulation.

A critical issue^{16-19,40} should be addressed before describing how we performed any MD simulation on a transition state structure. In principle, MD simulation using a classical force field (molecular mechanics) can only simulate a stable structure corresponding to a local minimum on the potential energy surface, whereas a transition state during a reaction process is always associated with a first-order saddle point on the potential energy surface. Hence, MD simulation using a classical force field cannot directly simulate a

transition state without any restraint on the geometry of the transition state. Nevertheless, in theory, if we can technically remove the degree of freedom corresponding to the imaginary vibration frequency in the transition state structure, then the number of the degrees of vibrational freedom (normal vibration modes) for a nonlinear molecule will decrease from $3N - 6$ to $3N - 7$. The transition state structure is associated with a local minimum on the potential energy surface within a subspace of the reduced degrees of vibrational freedom (i.e., subspace of the $3N - 7$ degrees of freedom), although it is associated with a first-order saddle point on the potential energy surface with all of the $3N - 6$ degrees of vibrational freedoms. Theoretically, the degree of vibrational freedom associated with the imaginary vibrational frequency in the transition state structure can be removed by appropriately freezing the reaction coordinate. The reaction coordinate corresponding to the imaginary vibration of the transition state is generally characterized by a combination of some key geometric parameters. Thus, we just need to maintain the bond lengths of the forming and breaking covalent bonds during the MD simulation on a transition state.¹⁶ The forming and breaking covalent bonds in the transition state will be called "transition" bonds below for convenience. Specifically, for transition state structures TS1_{ben}-Re, TS1_{ben}-Si, and TS1_{met} depicted in Figure 4, the reaction coordinate is mainly related to the partial covalent bond (C-O) between the hydroxide oxygen and a carbonyl carbon of the cocaine. This C-O bond is considered to be a transition bond in this study. During the MD simulations on the systems involving TS1_{ben}-Re, TS1_{ben}-Si, or TS1_{met}, we just needed to fix the length of this transition bond along with other bond lengths involving the carbonyl carbon of the cocaine and bond angles centered on the carbonyl carbon of the cocaine, starting from the fully optimized transition state geometries at the B3LYP/6-31+G* level without antibody. All of the other geometric degrees of freedom were allowed to move during the MD simulations.

It should be pointed out that the only purpose of performing the above-mentioned MD simulation on a transition state is to estimate the interaction energy between the reaction center and the protein environment in the transition state. An implied approximation used in the MD simulations on a transition state is that the length of the transition bond and the related geometric parameters in the transition state do not significantly/dramatically change from the cocaine hydrolysis without antibody to the cocaine hydrolysis with the antibody. This approximation should be reasonable because there is no covalent bonding between the antibody and the transition state structure of cocaine hydrolysis. Even if the length of the transition bond and the related geometric parameters within the reaction center do change significantly, the interaction energy between the reaction center and the protein environment is not expected to change significantly, in light of our previous QM, MD, and QM/MM calculations/simulations on butyrylcholinesterase-catalyzed hydrolysis of cocaine.^{13,16,18}

To carry out the MD simulations, the topologic and coordinate files of the antibody-ligand complexes were built with LEap module of the Amber8 package. The Parm99.dat and gaff.dat files of the Amber force field^{41,42} were used for the antibody and ligands, respectively. The force field parameters and RESP charges used for the noncommon atoms of the ligands are provided in the Supporting Information. The cocaine-antibody complex has a net charge of -3, whereas each TS1-antibody complex has a net charge of -4. Each complex was neutralized by adding three or four sodium counterions and was solvated in a rectangular box of TIP3P water molecules⁴³ with a solute wall distance of 10 Å. The energy minimization and MD simulation were performed by using

(31) Bernstein, F. C.; Koetzle, T. F.; Williams, G. J.; Meyer, E. F., Jr.; Brice, M. D.; Rodgers, J. R.; Kennard, O.; Shimanouchi, T.; Tasumi, M. *J. Mol. Biol.* **1977**, *112*, 535.

(32) Frisch, M. J. *Gaussian 03*, revision A.1; Gaussian, Inc.: Pittsburgh, PA, 2003.

(33) Singh, U. C.; Kollman, P. A. *J. Comput. Chem.* **1984**, *5*, 129.

(34) Besler, B. H.; Merz, K. M.; Kollman, P. A. *J. Comput. Chem.* **1990**, *11*, 431.

(35) Bayly, C. I.; Cieplak, P.; Cornell, W. D.; Kollman, P. A. *J. Phys. Chem.* **1993**, *97*, 10269.

(36) Cornell, W. D.; Cieplak, P.; Bayly, C. I.; Kollman, P. A. *J. Am. Chem. Soc.* **1993**, *115*, 9620.

(37) Case, D. A.; *AMBER 8*; University of California: San Francisco, 2004.

(38) Morris, G. M.; Goodsell, D. S.; Halliday, R. S.; Huey, R.; Hart, W. E.; Belew, R. K.; Olson, A. J. *J. Comput. Chem.* **1998**, *19*, 1639.

(39) Morris, G. M.; Goodsell, D. S.; Huey, R.; Hart, W. E.; Halliday, R. S.; Belew, R.; Olson, A. *J. AutoDock*, version 3.0.5; La Jolla, CA, 2001.

(40) Eksterowicz, J. E.; Houk, K. N. *Chem. Rev.* **1993**, *93*, 2439.

(41) Wang, J. M.; Wolf, R. M.; Caldwell, J. W.; Kollman, P. A.; Case, D. A. *J. Comput. Chem.* **2004**, *25*, 1157.

(42) Wang, J. M.; Cieplak, P.; Kollman, P. A. *J. Comput. Chem.* **2000**, *21*, 1049.

(43) Jorgensen, W. L.; Chandrasekhar, J.; Madura, J. D.; Impey, R. W.; Klein, M. L. *J. Chem. Phys.* **1983**, *79*, 926.

the Sander module of the Amber8 package in the way similar to what we did for other protein–ligand systems.^{13–16,18,19,44–48} First, the solvent molecules were minimized for 5000 cycles and equilibrated for 10 ps to make sure that they were in an equilibrated condition. Second, the solvent, ligand, and side chains of the antibody were allowed to move during a 1000 cycle energy minimization to adjust the positions of the ligand atoms in the binding pocket. Then the whole system was energy-minimized for 1000 cycles. This system was gradually heated from $T = 10$ K to $T = 100$ K for 20 ps before the MD simulation at 100 K for 1.2 ns in order to further relax the antibody–ligand binding and obtain the best possible binding structure. To obtain the best possible binding mode, the available intermolecular hydrogen bonds formed after the energy minimization were restrained during the heating and the first 200 ps of the MD simulation at 100 K, and then the whole complex was relaxed for 1 ns to obtain a stable MD trajectory. The time step used in the MD simulation was 2 fs. Periodic boundary condition was used in the NPT ensemble with Berendsen temperature coupling and $P = 1$ atm with isotropic molecular-based scaling. The SHAKE algorithm^{49,50} was used to fix all covalent bonds containing hydrogen atoms. The nonbonded pair list was updated every 25 steps. The particle mesh Ewald (PME) method was used to treat long-range electrostatic interactions;⁵¹ 10 Å was used as the nonbonded cutoff. During the MD simulation, the coordinates of the simulated complex were saved every 1 ps.

Binding Free Energy Calculation. The binding free energies between mAb15A10 and the ligands were calculated with a molecular mechanics–Poisson–Boltzmann surface area (MM–PBSA) method.⁵² In the MM–PBSA method, the free energy of the ligand binding with the antibody, ΔG_{bind} , is calculated from the difference between the free energy of the receptor–ligand complex (G_{cpx}) and the sum of the free energies of the unbound receptor (G_{rec}) and ligand (G_{lig}) as follows:

$$\Delta G_{\text{bind}} = G_{\text{cpx}} - (G_{\text{rec}} + G_{\text{lig}}) \quad (15)$$

The binding free energy ΔG_{bind} includes three items: MM gas-phase binding energy (ΔE_{MM}), solvation free energy (ΔG_{solv}), and entropy contribution ($-T\Delta S$). The sum of ΔE_{MM} and ΔG_{solv} is denoted by ΔE_{bind} . The MM gas-phase binding energy ΔE_{MM} was calculated with the Sander modules of the Amber8 program. The solvation free energy is the sum of the electrostatic solvation free energy (ΔG_{PB}) and the nonpolar solvation energy (ΔG_{np}). In detail, ΔG_{PB} was calculated with the finite-difference solution to the Poisson–Boltzmann (PB) equation implemented in the Delphi program^{53,54} by using the same RESP charges as used in the aforementioned molecular docking and MD simulations. The dielectric constants used for the solute and the solvent–water were 1 and 80, respectively. The MSMS program⁵⁵ was used to calculate solvent-accessible surface area (SASA) in eq 20 to obtain the nonpolar

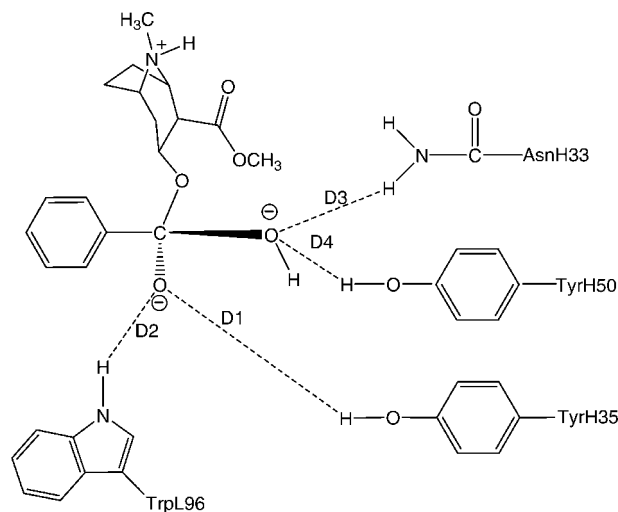


Figure 2. Schematic representation of TS1_{ben}–Re binding with the antibody. The dashed lines refer to the key distances between TS1_{ben}–Re and the antibody.

solvation energy, with parameters $\gamma = 0.00542$ kcal/Å² and $\beta = 0.92$ kcal/mol. We used the standard van der Waals radii^{56,57} built in the Amber program for solvation calculations.

$$\Delta G_{\text{bind}} = \Delta E_{\text{MM}} + \Delta G_{\text{solv}} - T\Delta S \quad (16)$$

$$\Delta E_{\text{bind}} = \Delta E_{\text{MM}} + \Delta G_{\text{solv}} \quad (17)$$

$$\Delta E_{\text{MM}} = \Delta E_{\text{ele}} + \Delta E_{\text{vdw}} \quad (18)$$

$$\Delta G_{\text{solv}} = \Delta G_{\text{PB}} + \Delta G_{\text{np}} \quad (19)$$

$$\Delta G_{\text{np}} = \gamma \text{SASA} + \beta \quad (20)$$

The entropy contribution to the binding free energy ($-T\Delta S$) was obtained by using a local program developed in our own laboratory. In this method, the entropy contribution is attributed to two contributions: solvation free entropy (ΔS_{solv}) and conformational free entropy (ΔS_{conf})

$$\Delta S = \Delta S_{\text{solv}} + \Delta S_{\text{conf}} \quad (21)$$

The solvation entropy is gained by the tendency of water molecules to minimize their contacts with hydrophobic groups in protein.⁵⁸ It has been demonstrated that the solvation entropy is temperature-dependent and can be calculated with heat capacity.^{59,60}

$$\Delta S_{\text{solv}} = \Delta C_{\text{p,ap}} \ln \frac{T}{T_{\text{S,ap}}^*} + \Delta C_{\text{p,pol}} \ln \frac{T}{T_{\text{S,pol}}^*} \quad (22)$$

where $\Delta C_{\text{p,ap}}$ and $\Delta C_{\text{p,pol}}$ are the apolar and polar heat capacity. $T_{\text{S,ap}}^*$ and $T_{\text{S,pol}}^*$ are the temperatures in which the apolar and polar hydration entropies are zero, and their values reported in the literature are 385.15⁶¹ and 335.15 K,⁶² respectively. The value of temperature T used in eq 22 was 298.15 K. For the calculation of apolar and polar heat capacities, the apolar and polar heat capacity changes for the protein–ligand binding can be expressed as a linear combination of apolar and polar solvent-accessible surface area differences $\Delta \text{SASA}_{\text{ap}}$ and $\Delta \text{SASA}_{\text{pol}}$.

$$\Delta C_{\text{p,ap}} = a_c(T) \Delta \text{SASA}_{\text{ap}} \quad (23)$$

(44) Hamza, A.; Cho, H.; Tai, H. H.; Zhan, C.-G. *Bioorg. Med. Chem.* **2005**, *13*, 4544.

(45) Hamza, A.; Zhan, C.-G. *J. Phys. Chem. B* **2006**, *110*, 2910.

(46) Koca, J.; Zhan, C.-G.; Rittenhouse, R. C.; Ornstein, R. L. *J. Am. Chem. Soc.* **2001**, *123*, 817.

(47) Koca, J.; Zhan, C.-G.; Rittenhouse, R. C.; Ornstein, R. L. *J. Comput. Chem.* **2003**, *24*, 368.

(48) Zhan, C.-G.; de Souza, O. N.; Rittenhouse, R.; Ornstein, R. L. *J. Am. Chem. Soc.* **1999**, *121*, 7279.

(49) Berendsen, H. J. C.; Postma, J. P. M.; Vangunsteren, W. F.; Dinola, A.; Haak, J. R. *J. Chem. Phys.* **1984**, *81*, 3684.

(50) Ryckaert, J. P.; Ciccoliti, G.; Berendsen, H. J. C. *J. Comput. Phys.* **1977**, *23*, 327.

(51) Essmann, U.; Perera, L.; Berkowitz, M. L.; Darden, T.; Lee, H.; Pedersen, L. G. *J. Chem. Phys.* **1995**, *103*, 8577.

(52) Kollman, P. A.; *Acc. Chem. Res.* **2000**, *33*, 889.

(53) Gilson, M. K.; Sharp, K. A.; Honig, B. H. *J. Comput. Chem.* **1988**, *9*, 327.

(54) Jayaram, B.; Sharp, K. A.; Honig, B. H. *Biopolymers* **1989**, *28*, 975.

(55) Sanner, M. F.; Olson, A. J.; Spehner, J. C. *Biopolymers* **1996**, *38*, 305.

(56) Bondi, A. *J. Phys. Chem.* **1964**, *68*, 441.

(57) Rowland, R. S.; Taylor, R. *J. Phys. Chem.* **1996**, *100*, 7384.

(58) Raha, K.; Merz, K. M., Jr. *J. Med. Chem.* **2005**, *48*, 4558.

(59) Bardi, J. S.; Luque, I.; Freire, E. *Biochemistry* **1997**, *36*, 6588.

(60) Gomez, J.; Freire, E. *J. Mol. Biol.* **1995**, *252*, 337.

(61) Baldwin, R. L. *Proc. Natl. Acad. Sci. U.S.A.* **1986**, *83*, 8069.

(62) D'Aquino, J. A.; Gomez, J.; Hilsner, V. J.; Lee, K. H.; Amzel, L. M.; Freire, E. *Proteins* **1996**, *25*, 143.

$$\Delta C_{p,\text{pol}} = b_c(T)\Delta S_{\text{ASA}}_{\text{pol}} \quad (24)$$

where $a_c(T)$ and $b_c(T)$ are temperature-dependent coefficients. In a low temperature ($T < 353$ K) situation, the heat capacities can be seen as temperature-independent, and the values of $a_c(T)$ and $b_c(T)$ reported in the literature are 0.45 and -0.26 , respectively.⁶⁰

The conformational entropy (ΔS_{conf}) is related to the change of the number of rotatable bonds during the binding process. For a four-atom unit X–A–B–Y, if the middle bond A–B is a nonbackbone single bond with at least one carbon atom among A and B and neither of the atoms X and Y is hydrogen, it is regarded as a rotatable bond. In the binding site of the protein in the protein–ligand complex, if any one of the four atoms involved in a rotatable bond in the protein/ligand is within a distance of 6 Å from any of the ligand/protein atoms, this bond will be regarded as nonrotatable. The contribution to the binding free energy from the conformational entropy change is proportional to the number (ΔN_{rot}) of the lost rotatable bonds during the binding:⁵⁸

$$-T\Delta S_{\text{conf}} = w(\Delta N_{\text{rot}}) \quad (25)$$

in which w is the scaling factor to be calibrated. Hence, our MM–PBSA calculations include an adjustable parameter (i.e., w) in the calculation of the free energy contribution from the conformational entropy

$$\begin{aligned} \Delta G_{\text{bind}} &= \Delta E_{\text{bind}} - T\Delta S_{\text{solv}} - T\Delta S_{\text{conf}} \\ &= \Delta E_{\text{bind}} - T\Delta S_{\text{solv}} + w(\Delta N_{\text{rot}}) \quad (26) \end{aligned}$$

although all of the other parameters used in our MM–PBSA calculations are the standard parameters reported in literature or the default parameters of the Amber8 program. This adjustable parameter, w , was calibrated to be 0.8452 kcal/mol (when four effective digits were kept) by fitting the calculated ΔG_{bind} value for the cocaine–antibody binding to the corresponding experimental ΔG_{bind} value of -4.97 kcal/mol determined by the K_M value of 220 μM . Thus, $w = 0.8452$ kcal/mol was used for our MM–PBSA calculations on all of the complexes in this study. We noticed that the w value of 0.8452 kcal/mol calibrated in the present study is slightly smaller than 1 kcal/mol obtained in a previous study.⁵⁸ The difference may be attributed to the possibility that different protein systems may need a slightly different w value to achieve their own best possible fits. Nevertheless, the use of a different w value would not qualitatively change the relative binding free energies for a protein binding with different ligands, as a slight change of the w value will only systematically (and almost uniformly) change the entropic contributions to the binding free energies for all of the ligands.

The final binding free energy ΔG_{bind} for each antibody–ligand binding complex was taken as the average of the ΔG_{bind} values calculated for 100 snapshots of the MD-simulated complex. The 100 snapshots were taken from the last 500 ps of the MD trajectory, with one snapshot for every 5 ps.

The MD simulations were performed on an HP supercomputer (Superdome with 256 shared-memory processors) or on an HP XC Linux cluster at the Center for Computational Sciences, University of Kentucky. The other computations were carried out on SGI Fuel workstations in our own laboratory.

Results and Discussion

Binding Structures. Depicted in Figures 1 to 4 are the schematic representations of the MD-simulated structures of mAb15A10 binding with the four different ligands, including cocaine, TS1_{ben}–Re, TS1_{ben}–Si, and TS1_{met}. As shown in the figures, the antibody binds with cocaine, TS1_{ben}–Re, TS1_{ben}–Si, and TS1_{met} mainly through some of four potential hydrogen bonds with the side chains of residues TyrH35, TrpL96, AsnH33, and TyrH50 (D1–D4, see Figure 4). The representative snapshots of the MD-simulated complexes are shown in Figures 5 to 8, giving the average H···O distances involved in

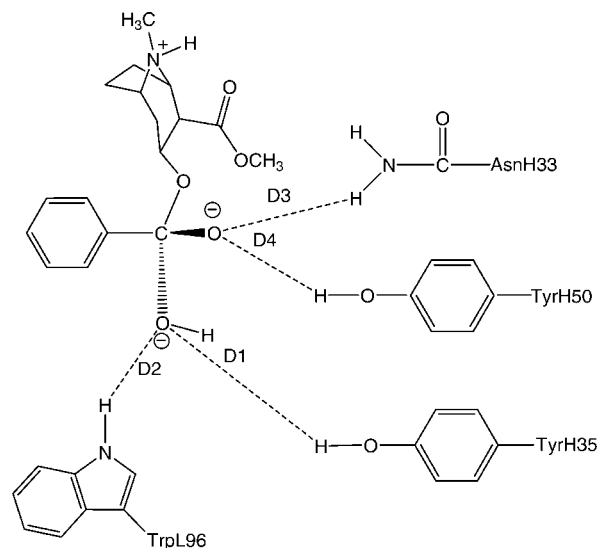


Figure 3. Schematic representation of TS1_{ben}–Si binding with the antibody. The dashed lines refer to the key distances between TS1_{ben}–Si and the antibody.

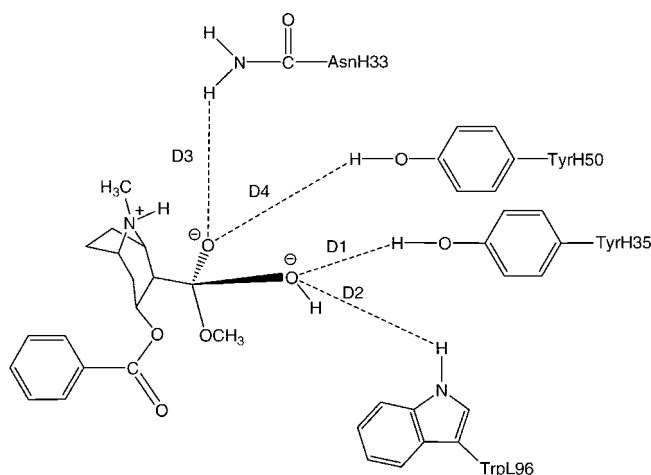


Figure 4. Schematic representation of TS1_{met} binding with the antibody. The dashed lines refer to the key distances between TS1_{met} and the antibody.

the hydrogen bonds between the antibody and ligand. Depicted in Figures 9 to 12 is the time dependence of the H···O distances (D1–D4) involving TyrH35, TrpL96, AsnH33, and TyrH50.

A survey of these figures reveals two hydrogen bonds for the antibody binding with cocaine, four hydrogen bonds with TS1_{ben}–Re, three hydrogen bonds with TS1_{ben}–Si, and two hydrogen bonds with TS1_{met}. For the antibody binding with cocaine (see Figures 1, 5, and 9), although there were three hydrogen bonds between the antibody and the carbonyl oxygen of cocaine benzoyl ester in the initial structure (obtained from molecular docking) used for the MD simulation, only two of the three hydrogen bonds (i.e., with the side chains of TyrH35 and TrpL96) were kept during the MD simulation. The hydrogen bond between AsnH33 side chain and the carbonyl oxygen of cocaine benzoyl ester was broken during the MD simulation. The AsnH33 side chain turned to form another hydrogen bond with a nearby water molecule. The average H···O distances of the two hydrogen bonds of cocaine with TyrH35 and TrpL96 are 1.92 and 1.93 Å, respectively.

For the antibody binding with TS1_{ben}–Re, as seen in Figures 6 and 10, all of the four hydrogen bonds (associated with

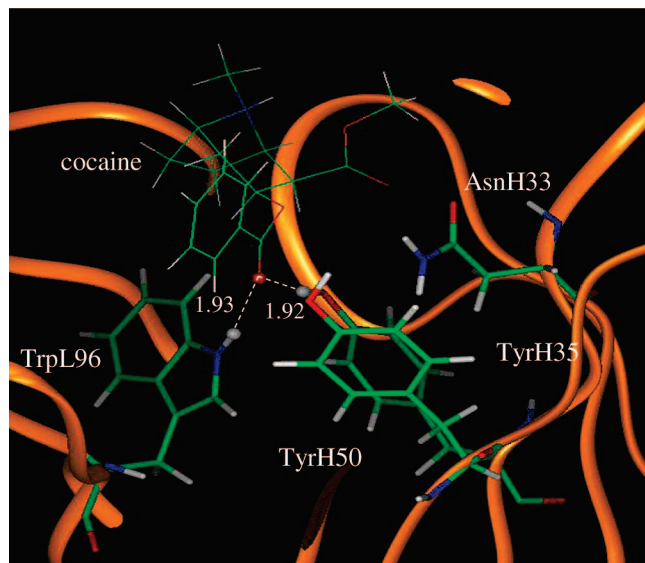


Figure 5. The MD simulated structure of cocaine binding with the antibody. The key distances indicated in the figure are the simulated average distance (Å).

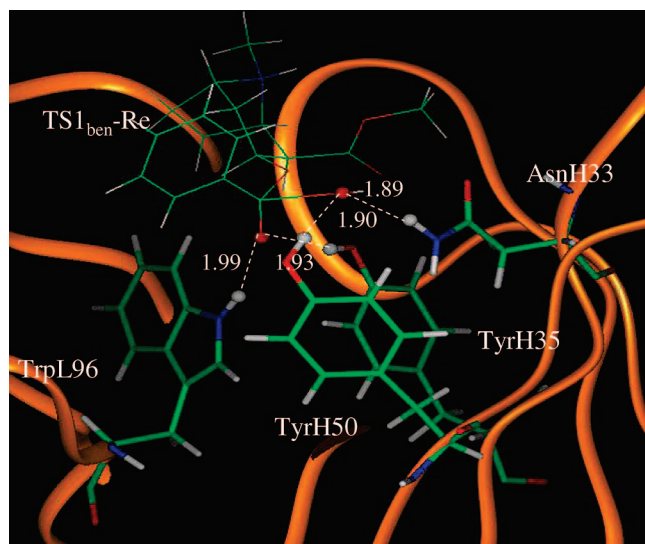


Figure 6. The MD simulated structure of TS1_{ben}-Re binding with the antibody. The key distances indicated in the figure are the simulated average distance (Å).

D1–D4 in Figure 2) in the initial structure were kept during the MD simulation, with the simulated average distances of 1.93, 1.99, 1.89, and 1.90 Å for D1, D2, D3, and D4, respectively. Compared to the two hydrogen bonds of the antibody binding with cocaine, the overall strength of the four hydrogen bonds in the antibody binding with TS1_{ben}-Re should be much stronger. For the antibody binding with TS1_{ben}-Si, as seen in Figures 7 and 11, three hydrogen bonds associated with D1–D3 (see Figure 3) existed in both the initial structure and the MD-simulated structure. The MD-simulated average D1, D2, and D3 values are 1.64, 1.83, and 1.93 Å, respectively. Compared to the antibody binding with TS1_{ben}-Re, the antibody binding with TS1_{ben}-Si did not involve a hydrogen bond between TS1_{ben}-Si and TyrH50. The overall strength of the three hydrogen bonds in the antibody binding with TS1_{ben}-Si should also be stronger than that with cocaine. Thus, the transition states

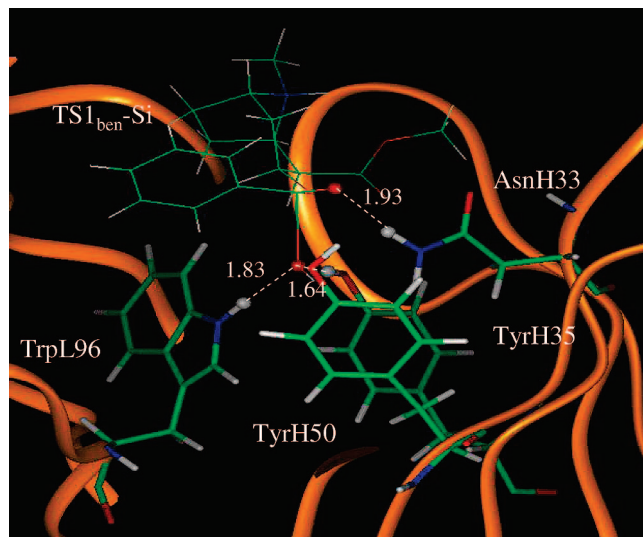


Figure 7. The MD simulated structure of TS1_{ben}-Si binding with the antibody. The key distances indicated in the figure are the simulated average distance (Å).

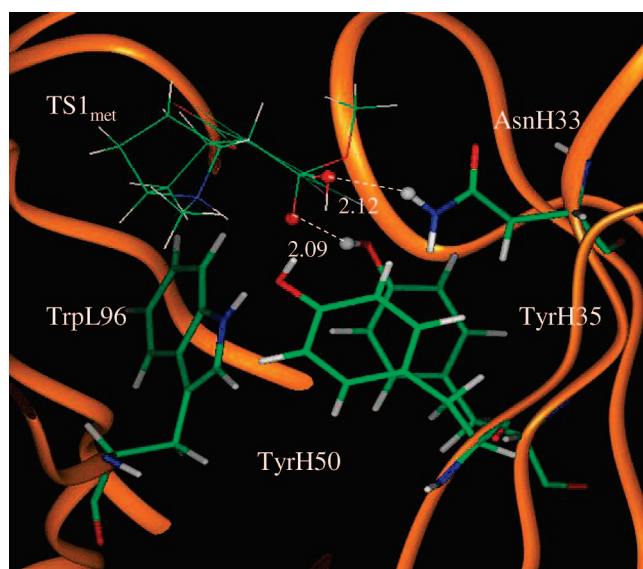


Figure 8. The MD simulated structure of TS1_{met} binding with the antibody. The key distances indicated in the figure are the simulated average distance (Å).

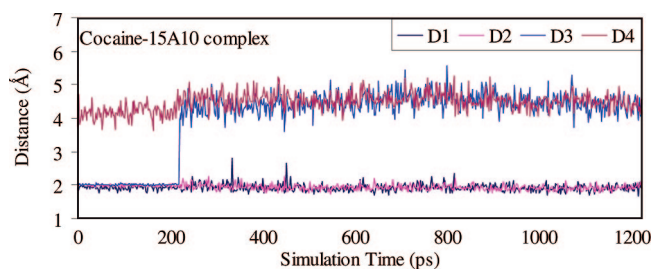


Figure 9. Plots of the key internuclear distances versus the simulation time for cocaine binding with the antibody. See Figure 1 for the definitions of distances D1, D2, D3, and D4.

TS1_{ben}-Re and TS1_{ben}-Si are expected to be stabilized by the antibody relative to the cocaine binding with the same antibody.

However, for the antibody binding with TS1_{met}, the MD simulation only revealed two weak hydrogen bonds (corre-

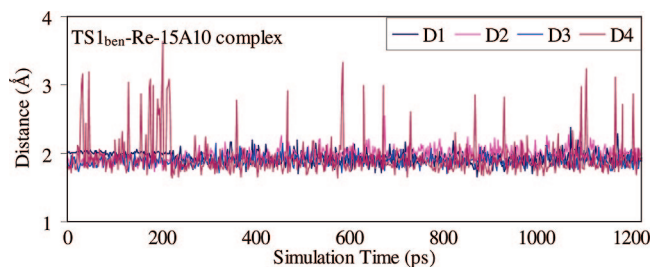


Figure 10. Plots of the key internuclear distances versus the simulation time for $TS1_{ben}-Re$ binding with the antibody. See Figure 2 for the definitions of distances D1, D2, D3, and D4.

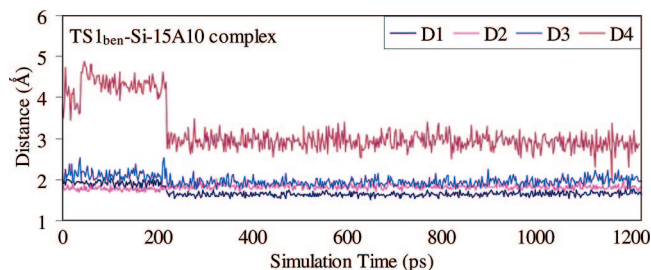


Figure 11. Plots of the key internuclear distances versus the simulation time for $TS1_{ben}-Si$ binding with the antibody. See Figure 3 for the definitions of distances D1, D2, D3, and D4.

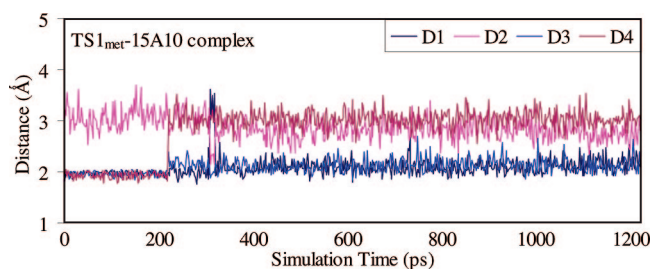


Figure 12. Plots of the key internuclear distances versus the simulation time for $TS1_{met}$ binding with the antibody. See Figure 4 for the definitions of distances D1, D2, D3, and D4.

sponding to D1 and D3 in Figure 4) with the side chains of TyrH35 and AsnH33. The overall strength of the two hydrogen bonds in the antibody binding with $TS1_{met}$ should be weaker than that of the two hydrogen bonds in the cocaine–antibody binding, due to the longer $H\cdots O$ distances (2.09 and 2.12 Å in the $TS1_{met}$ –antibody binding versus 1.92 and 1.93 Å in the cocaine–antibody binding). Thus, the transition state $TS1_{met}$ is not expected to be stabilized by the antibody relative to the cocaine binding with the antibody.

It should be pointed out that the above discussion on the hydrogen bonds has ignored the hydrogen bond angles that should also affect the strengths of the hydrogen bonds. We actually checked the hydrogen bond angles ($\angle OHO$ or $\angle OHN$) associated with the aforementioned hydrogen bonds and found that all of the MD-simulated average hydrogen bond angles are all within ~ 150 to 170° , suggesting that these hydrogen bonds were not bent considerably during the MD simulations. The plots for the time dependence of the hydrogen bond angles are provided in the Supporting Information.

A remarkable feature of the simulated structures is that, in addition to the previously recognized residues TyrH35, TrpL96, and AsnH33 that could form the oxyanion hole, TyrH50 is also

important for stabilizing the transition state $TS1_{ben}-Re$ as TyrH50 forms a strong hydrogen bond with transition state $TS1_{ben}-Re$.

Binding Free Energies. Summarized in Table 1 are the binding free energies calculated with the MM–PBSA approach for the antibody binding with cocaine, $TS1_{ben}-Re$, $TS1_{ben}-Si$, and $TS1_{met}$. As seen in the table, the calculated entropy contributions for the four complexes are close to each other, with values ranging from 13.03 to 14.56 kcal/mol. This is reasonable because the entropic contribution is mainly determined by the sizes and shapes of the antibody and ligand involved in the binding. The calculated van der Waals contributions to the binding free energies for all of the complexes, except for $TS1_{met}$, are also very close to each other, ranging from -27.56 to -28.24 kcal/mol. This is because the binding modes in the three complexes (with cocaine, $TS1_{ben}-Re$, and $TS1_{ben}-Si$) are similar. For the complex with $TS1_{met}$, the van der Waals contribution (-35.79 kcal/mol) is significantly more favorable due to the remarkably different binding mode. In $TS1_{met}$, it is the methyl ester group (rather than the benzoyl ester group) with the hydroxide ion that interacts with the binding site of the antibody. A careful check of the simulated binding structure reveals that the more favorable van der Waals energy associated with $TS1_{met}$ may be attributed to the favorable position of $TS1_{met}$. In the simulated antibody– $TS1_{met}$ binding structure, the tropane ring of $TS1_{met}$ was sandwiched between the side chains of residues TrpL91 and TrpL96. The calculated electrostatic contributions to the binding free energies for the four complexes are quite different, with -93.09 , -44.57 , -65.91 , and -11.45 kcal/mol for cocaine, $TS1_{ben}-Re$, $TS1_{ben}-Si$, and $TS1_{met}$, respectively. Correspondingly, the solvation shifts calculated for the four complexes are also very different, ranging from 32.71 to 103.19 kcal/mol. Overall, the binding free energies calculated for the antibody binding with cocaine, $TS1_{ben}-Re$, $TS1_{ben}-Si$, and $TS1_{met}$ are -4.97 , -11.84 , -10.70 , and -0.03 kcal/mol, respectively. The calculated binding free energy of -4.97 kcal/mol for the antibody binding with cocaine is consistent with the binding free energy of -4.97 kcal/mol estimated from the experimental K_M value of 220 μM .

Free Energy Barriers and Rate Acceleration. On the basis of the calculated binding free energies, the free energy barrier shift, $\Delta\Delta G_{av}$, from the cocaine hydrolysis in water to the antibody-catalyzed cocaine hydrolysis was evaluated for each reaction pathway. As seen in Table 2, the free energy barrier shifts calculated for the reaction pathways associated with $TS1_{ben}-Re$, $TS1_{ben}-Si$, and $TS1_{met}$ are -6.87 , -5.73 , and 5.00 kcal/mol, respectively. So, mAb15A10 significantly stabilizes the transition states for the hydrolysis of cocaine benzoyl ester, whereas it significantly destabilizes the transition state for the hydrolysis of cocaine methyl ester, relative to the cocaine–antibody binding. On the basis of our previous first-principles electronic structure calculations accounting for the solvent effects,²⁰ the free energy barriers for the reaction pathways associated with $TS1_{ben}-Re$, $TS1_{ben}-Si$, and $TS1_{met}$ of the cocaine hydrolysis in water in the physiologic pH (7.4) should be 25.9, 28.6, and 20.1 kcal/mol, respectively. On the basis of the previously calculated free energy barriers and the barrier shifts calculated in the present study, the free energy barriers for the reaction pathways associated with $TS1_{ben}-Re$, $TS1_{ben}-Si$, and $TS1_{met}$ of the antibody-catalyzed cocaine hydrolysis are predicted to be 19.0, 22.9, and 25.1 kcal/mol, respectively. These energetic results show that the dominant reaction pathway for the antibody-catalyzed cocaine hydrolysis

Table 1. Energetic Results (kcal/mol) Obtained from the MM–PBSA Calculations at $T = 298.15$ K and $P = 1$ atm for the Antibody Binding with Cocaine, TS1_{ben}–Re, TS1_{ben}–Si, and TS1_{met}

ligand in the complex	calcd ^a						exptl ^b	
	ΔE_{ele}	ΔE_{vdw}	ΔE_{MM}	ΔG_{solv}	ΔE_{bind}	$-T\Delta S$	ΔG_{bind}	ΔG_{bind}
cocaine	−93.09 (2.13)	−28.10 (1.27)	−121.20 (2.08)	103.19 (1.99)	−18.00 (2.03)	13.03 (0.62)	−4.97 (1.50)	−4.97
TS1 _{ben} –Re	−44.57 (4.58)	−27.56 (1.50)	−72.13 (3.93)	47.00 (2.99)	−25.13 (3.49)	13.29 (1.03)	−11.84 (2.57)	
TS1 _{ben} –Si	−65.91 (3.59)	−28.24 (1.94)	−94.16 (2.67)	71.17 (2.23)	−22.99 (2.46)	12.29 (1.02)	−10.70 (1.88)	
TS1 _{met}	−11.45 (2.55)	−35.79 (0.93)	−47.24 (2.52)	32.71 (1.95)	−14.53 (2.25)	14.56 (0.89)	−0.03 (1.71)	

^a The numbers in the parentheses refer to the root-mean-square fluctuation (RMSF) of the calculated energetic values. ^b Estimated from the experimental K_M value of 220 μM reported in ref 6.

Table 2. Free Energy Barriers (ΔG_{av} in kcal/mol) Calculated for Three Competing Reaction Pathways of the Cocaine Hydrolysis

reaction pathway	$\Delta G_{\text{av}}(\text{aq})$ (SRS) ^a	$\Delta G_{\text{av}}(\text{aq})$ (pH 7.4) ^b	$\Delta\Delta G_{\text{av}}^c$	$\Delta G_{\text{av}}(\text{antibody})$ (pH 7.4) ^d
cocaine + HO [−] → TS1 _{ben} –Re	16.9	25.9	−6.87 (−5.93)	19.0
cocaine + HO [−] → TS1 _{ben} –Si	19.6	28.6	−5.73	22.9
cocaine + HO [−] → TS1 _{met}	11.1	20.1	5.00	25.1

^a Free energy barriers determined by the first-principles electronic structure calculations (ref 20) for the cocaine hydrolysis in water using the standard reference state (SRS), that is, 1 M, for all molecular species, including [HO[−]] = 1 M, at $T = 298.15$ K. ^b Free energy barriers determined for the cocaine hydrolysis in water at the physiologic pH (7.4) at $T = 298.15$ K. The free energy barrier shift from the standard reference state of [HO[−]] = 1 M to pH 7.4 is 9.0 kcal/mol when $T = 298.15$ K. ^c The free energy barrier shift from the cocaine hydrolysis in water to the antibody-catalyzed cocaine hydrolysis (determined by using the data in Table 1). The value −5.93 kcal/mol in parentheses was the free energy barrier shift derived from the experimental rate acceleration ($k_{\text{cat}}/k_0 = 23\,000$) using eq 13. ^d Free energy barriers calculated for the antibody-catalyzed cocaine hydrolysis at the physiologic pH (7.4) at $T = 298.15$ K.

is associated with transition state TS1_{ben}–Re, although the dominant reaction pathway for the cocaine hydrolysis in water is associated with transition state TS1_{met}.

Further, when you only consider cocaine hydrolysis at the benzoyl ester, the reaction pathway with the lowest free energy barrier is always associated with transition state TS1_{ben}–Re for both the cocaine hydrolysis in water and the antibody-catalyzed cocaine hydrolysis. Hence, for the hydrolysis of cocaine benzoyl ester, the calculated free energy barrier shift of −6.87 kcal/mol can directly be compared with the experimental rate acceleration ($k_{\text{cat}}/k_0 = 23\,000$).⁶ According to eq 13, when the rate acceleration (k_{cat}/k_0) is 23 000, the corresponding free energy barrier shift should be −5.93 kcal/mol at $T = 298.15$ K. The experimentally derived free energy barrier shift of −5.93 kcal/mol is close to the calculated free energy barrier shift of −6.87 kcal/mol. In light of the good agreement between the calculated energetic results and available experimental data, it should be interesting to employ the same computational protocol to calculate the free energy barriers for the cocaine hydrolysis catalyzed by various mutants of the anticocaine catalytic antibody for future rational design of possible high-activity mutants of the catalytic antibody against cocaine.

For further validation, the same computational protocol (with the above-calibrated w value of 0.8452 kcal/mol) was also used to examine the cocaine hydrolysis catalyzed by two antibody mutants (i.e., AsnH33Ala and TyrH35Phe) for which the relative experimental activity data are available. Here, mutation AsnH33Ala means that the Asn33 residue of the high chain is changed to Ala residue, whereas mutation TyrH35Phe means that the Tyr35 residue of the high chain is changed to Phe

residue. The MD trajectories and the simulated binding structures are provided as Supporting Information. The calculated energetic results are summarized in Tables 3–5, in comparison with available experimental data. As seen in Table 5, the calculated shift of the free energy barrier from the wild-type antibody to the TyrH35Phe mutant is 2.46 kcal/mol, which is qualitatively consistent with the experimental free energy barrier shift, 0.85 kcal/mol, derived from the reported activity change from 100 to 24%.⁶ The calculated shift of the free energy barrier from the wild-type antibody to the AsnH33Ala mutant is 5.22 kcal/mol, which is also consistent with the experimental observation⁶ that the catalytic activity of the AsnH33Ala mutant was 0% (i.e., <0.5%) of the wild-type against cocaine. The activity change from 100 to <0.5% is associated with a free energy barrier change of >3.14 kcal/mol. Hence, the calculated mutation-caused shifts of the free energy barrier are also reasonably close to the available experimental activity data.

We note that the entropic contribution, 7.97 kcal/mol, calculated for TyrH35Phe binding with TS1_{ben}–Re is significantly lower than those calculated for all of the other antibody–ligand binding complexes involved in this study. The lower entropy contribution calculated for TyrH35Phe binding with TS1_{ben}–Re is mainly attributed to the significantly lower contribution from the solvation entropy change, although the calculated contribution from the conformational entropy change is also lower. The detailed results of the entropic contributions are provided in the Supporting Information.

Conclusion

The free energy barriers for the competing reaction pathways of the cocaine hydrolysis catalyzed by an anti-cocaine catalytic antibody, mAb15A10, were predicted, in the present study, by using a novel computational strategy based on the binding free energy calculations on the antibody binding with cocaine and the transition states. On the basis of the calculated binding free energies, we were able to evaluate the free energy barrier shift from the cocaine hydrolysis in water to the antibody-catalyzed cocaine hydrolysis for each reaction pathway. The free energy barriers for the antibody-catalyzed cocaine hydrolysis were predicted to be the corresponding free energy barriers for the cocaine hydrolysis in water plus the calculated free energy barrier shifts. On the basis of the predicted free energy barriers, the dominant reaction pathway for the antibody-catalyzed cocaine hydrolysis was determined. The calculated free energy barrier shift of −6.87 kcal/mol from the dominant reaction pathway of the cocaine benzoyl ester hydrolysis in water to the dominant reaction pathway of the antibody-catalyzed hydrolysis of cocaine benzoyl ester is in good agreement with the experimentally derived free energy barrier shift of −5.93 kcal/mol (corresponding to the experimental rate acceleration $k_{\text{cat}}/k_0 = 23\,000$), while the calculated binding free energy of −4.97 kcal/mol for the cocaine–antibody binding is consistent with

Table 3. Energetic Results (kcal/mol) Obtained from the MM–PBSA Calculations at $T = 298.15$ K and $P = 1$ atm for the Cocaine Binding with the Antibody Mutants

antibody	ΔE_{ele}^a	ΔE_{vdw}	ΔE_{MM}	ΔG_{solv}	ΔE_{bind}	$-T\Delta S$	ΔG_{bind}
AsnH33Ala	-85.77 (2.17)	-26.13 (1.22)	-111.90 (2.02)	94.83 (2.02)	-17.07 (2.02)	12.46 (1.17)	-4.61 (1.65)
TyrH35Phe	-80.7 (2.02)	-29.01 (1.10)	-109.72 (2.07)	93.23 (1.95)	-16.49 (2.01)	12.83 (0.89)	-3.66 (1.55)

^a The numbers in the parentheses refer to the root-mean-square fluctuation (RMSF).

Table 4. Energetic Results (kcal/mol) Obtained from the MM–PBSA Calculations at $T = 298.15$ K and $P = 1$ atm for the TS1_{ben}–Re Binding with the Antibody Mutants

antibody	ΔE_{ele}^a	ΔE_{vdw}	ΔE_{MM}	ΔG_{solv}	ΔE_{bind}	$-T\Delta S$	ΔG_{bind}
AsnH33Ala	-32.94 (2.95)	-26.86 (1.57)	-59.80 (2.49)	40.98 (3.06)	-18.82 (2.79)	12.56 (1.13)	-6.26 (2.13)
TyrH35Phe	-46.62 (2.57)	-29.46 (1.33)	-76.08 (2.52)	60.04 (2.58)	-16.04 (2.61)	7.97 (1.19)	-8.07 (2.03)

^a The numbers in the parentheses refer to the root-mean-square fluctuation (RMSF).

Table 5. Mutation-caused shifts of free energy barrier (ΔG_{av} in kcal/mol) calculated for cocaine hydrolysis catalyzed by the antibody mutants in comparison with available experimental data.

antibody	calcd		exptl	
	$\Delta\Delta G_{\text{av}}^a$	relative ΔG_{av}^b	relative activity ^c	relative ΔG_{av}^b
wild-type	-6.87	0	100%	0
AsnH33Ala	-1.65	5.22	0% (i.e., < 0.5%)	> 3.14
TyrH35Phe	-4.41	2.46	24%	0.85

^a The free energy barrier shift from the cocaine hydrolysis in water to the antibody-catalyzed cocaine hydrolysis corresponding to the wild-type antibody and its mutants. ^b Mutation-caused shift of the free energy barrier (i.e., $\Delta\Delta G_{\text{av}} = \Delta\Delta G_{\text{av}}(\text{wild-type})$). The experimental shifts are derived from the experimental relative activity data (i.e., <0.5 and 24%). ^c Experimental activity of the mutant relative to the wild-type antibody (data from ref 6).

the experimentally derived binding free energy of -4.97 kcal/mol (estimated from the experimental K_M value of $220 \mu\text{M}$). The calculated mutation-caused shifts of the free energy barrier are also reasonably close to the available experimental activity data.

In light of the good agreement between the calculated energetic results and available experimental kinetic data, the computational protocol for calculating the free energy barrier shift from the cocaine hydrolysis in water to the antibody-catalyzed cocaine hydrolysis may be useful in future rational design of possible high-activity mutants of the catalytic antibody

as anti-cocaine therapeutics. The general computational strategy for calculating the free energy barrier shift may also be valuable for studying a variety of chemical reactions catalyzed by other antibodies or proteins through noncovalent bonding interactions with the substrates.

Acknowledgment. The research was supported by NIH/NIDA (Grant R01 DA013930 to C.-G.Z.). The authors also acknowledge the Center for Computational Sciences (CCS) at University of Kentucky for supercomputing time on HP Superdome (with 4 nodes and 256 processors) and on IBM X-series Cluster (with 34 nodes and 1360 processors).

Supporting Information Available: Sixteen figures for the MD trajectories (including plots for some key distances and angles versus the simulation time) and the simulated structures for the mutants of the catalytic antibody binding with cocaine and the transition states; a table for the contributions of the solvation entropy and conformational entropy to the binding free energies; the parameters used for the noncommon atom types in the transition state structures; the RESP charges used for the atoms in the transition state structures; complete citations of refs 10, 32, 37, and 52. This material is available free of charge via the Internet at <http://pubs.acs.org>.

JA077972S